Available online at www.sciencedirect.com

ScienceDirect

journal homepage: www.elsevier.com/locate/nanoenergy

RAPID COMMUNICATION

Voltage recovery in charged InAs/GaAs quantum dot solar cells

CrossMark

Phu Lam[a,1]**, Sabina Hatch**[a,1]**, Jiang Wu**[a,*,1]**, Mingchu Tang**[a]**, Vitaliy G. Dorogan**[b]**, Yuriy I. Mazur**[b]**, Gregory J. Salamo**[b]**, Iñigo Ramiro**[a,c]**, Alwyn Seeds**[a]**, Huiyun Liu**[a]

[a]*Department of Electronic and Electrical Engineering, University College London, Torrington Place, London WC1E 7JE, United Kingdom*
[b]*Institute for Nanoscience and Engineering, University of Arkansas, Fayetteville, Arkansas 72701, United States of America*
[c]*Instituto de Energía Solar, ETSI Telecomunicación, Avda. Complutense 30, 28040 Madrid, Spain*

Abstract
The realization of high efficiency quantum dot intermediate band solar cells is challenging due to the thermally activated charge escaping at high temperatures. The enhancement in short circuit current of quantum dot solar cells is largely undermined by the voltage loss. In this paper, InAs/GaAs quantum dot solar cells with direct Si doping in the quantum dots are studied. The open circuit voltage is improved with increasing doping concentration in the quantum dots. The recovery of open circuit voltage as large as 105 mV is measured. This voltage recovery is attributed to suppressed charge thermal escaping from quantum dots. The suppressed thermal coupling is supported by the external quantum efficiency and photoluminescence measurements.
© 2014 The Authors. Published by Elsevier Ltd. This is an open access article under the CC BY license (http://creativecommons.org/licenses/by/3.0/).

Introduction

The concept of introducing an intermediate band (IB) to increase the efficiency limit of a single-gap solar cell (SC) to 63.2% was proposed by Luque and Martí in 1997 [1]. The IB is predicated to significantly improve the photocurrent via multi-photon absorption, while at the same time conserve

*Corresponding author.
  E-mail address: jiang.wu@ucl.ac.uk (J. Wu).
[1]These authors contributed equally to this work.

the output voltage. Among the various efforts involved in the development of IBSCs, zero-dimensional quantum dots (QDs) with nominally discrete density of states have attracted much attention [2-6]. The discrete energy levels in the QDs can be employed as an IB and the electron ground states in the QDs are tentatively designated as the IB. For optimal SC performance, the IB is situated between the valence band (VB) and conduction band (CB) such that the absorption through the three transitions (VB→IB, IB→CB, and VB→CB) may result in cell efficiency exceeding the Shockley-Queisser limit [7]. One of the main challenges that have prevented the QD-IBSC from functioning effectively is the thermal coupling of IB and CB states [8]. This occurs when carriers have the ability to transition between the IB and CB via thermal excitation and relaxation, hence removing the need for two-photon excitation [9,10]. Subsequently, the split of quasi-Fermi levels for IB and CB can not form. This results in a reduced open-circuit voltage (V_{OC}), which is often observed for QD-IBSCs, and hence lowers the overall efficiency of the device [11,12]. Therefore, thermal decoupling between IB and CB in QDSC is of critical importance to realize the potential efficiency theoretically predicted for IBSC. To this end, Tutu et al. have reported recovery of V_{OC} via removal of the wetting layer (WL) that assist the thermal escape of electrons in quantum dots [13]. Ramiro et al. have also reported an InAs/Al$_{0.25}$Ga$_{0.75}$As QD-IBSC with thermal activation energy $\sim$140 meV higher than an InAs/GaAs QD-IBSC [14]. The higher conduction band offset between InAs and Al$_{0.25}$Ga$_{0.75}$As suppresses the carrier thermal escape up to 220 K. However, the carrier thermal escape and hence voltage loss is still significant at room temperature [13,14].

In this article, we report an alternative approach to inhibit the thermal coupling between the IB and CB which is detrimental to achieving intermediate band solar cells. We directly doped the conventional InAs/GaAs QDs with silicon with the aim of quenching the thermal transitions that occur between the IB and CB. By intentionally applying Si dopants to QDs, it forms a built-in field at the QD/WL interface. This increases the thermal activation energy of confined carriers and consequently reduces the thermal communication of carriers between the IB and CB. A voltage recovery as high as 105 mV at room temperature has been achieved with a Si doping density of 18 electrons (18e) per QD. Without using any high bandgap material, this method has achieved a voltage recovery similar to the start-of-the-art QDSCs [11]. We use both steady-state photoluminescence (PL) and transient PL spectroscopy to provide evidence that corroborates our theory and experimental observations. By simply designing the doping profile in the QD region, an internal electrical field can be created and suppress the thermal-assisted carrier escaping from the confined states in the QDs. This concept can also be applied to other kinds of quantum dot solar cells, such as high density QDSCs and strain-balanced QDSCs [11,16], to achieve high efficiency solar cells exceeding their bulk counterparts.

Experimental

All the epitaxial structures were grown by a solid-source molecular beam epitaxy (MBE) on n$^+$-GaAs (100) substrates.

All QDSCs had a p-i-n structure consisting of a 200 nm GaAs buffer layer with Si doping density of 1×10^{18} cm^{-3}, 1000 nm GaAs base with Si doping density of 1×10^{17} cm^{-3}, 420 nm intrinsic region, 250 nm GaAs emitter with Be doping density of 2×10^{18} cm^{-3}, 30 nm InGaP window layer with Be doping density of 2×10^{18} cm^{-3}, and 50 nm GaAs contact layer with Be doping density of 1×10^{19} cm^{-3}. The intrinsic region of the QDSCs contained 20 stacks of QD layers separated by a 20 nm GaAs spacer. The QDs were grown by the Stranski-Krastanov mode at substrate temperature of $\sim$470 °C measured by a pyrometer. High-growth-temperature GaAs spacer layers were applied during growth of QDs to suppress the formation of dislocations. During QD growth, direct Si-doping was carried out with dopant densities of 0, 6, 12, 18, and 24 electrons per QD and the QDSCs were named as 0e, 6e, 12e, 18e, and 24e QDSCs, accordingly. The doping density is calibrated using a QD sheet density of $\sim 3.0 \times 10^{10}$ cm^{-2} measured from atomic force microscope (AFM) (see Supporting information, Figure S1). Two GaAs reference SCs share the same growth conditions without QDs with one being GaAs reference SC and another being 18e GaAs SC, which was doped in the intrinsic region same as the 18e QDSC.

Post-MBE growth, the SCs were cleaned using acetone for 10 mins in an ultrasonic bath, the process was then repeated with isopropanol. To remove surface oxidation, the SC was immersed for 20 s in a 1:1 solution of concentrated hydrochloric acid and deionized water before rinsing in deionized water and dried with nitrogen. A gold-zinc alloy was thermally evaporated to form a grid-pattern p-type electrode with the use of a metal mask. The thermally evaporated n-type electrode coated the whole surface and consisted of nickel/gold-germanium/nickel/gold (5 nm/150 nm/50 nm/200 nm thicknesses, respectively). No anti-reflection coating was deposited in the fabrication of the QDSCs.

Current density vs. voltage (J-V) measurements were performed under one sun (AM 1.5G) illumination using a LOT calibrated solar simulator with a Xeon lamp. A 4-point probe station was used to connect the devices to a Keithly 2400 sourcemeter that output the data to Photor 3.1 software. Photocurrent measurements were obtained with a Halogen lamp chopped to a frequency of 188 Hz through a Newport monochromator, a 4-point probe in connection with a lock-in amplifier was used to collect data. The monochromatic beam was calibrated using a Silicon photodiode and the data analyzed with Tracer 3.2 software to produce the external quantum efficiency (EQE).

Steady-state photoluminescence (PL) measurements were performed using 532 nm excitation from a Nd:YAG laser with a spot diameter of 20 μm and an unfocused diode-pumped solid-state laser. Transient PL measurements used 2 ps pulses at excitation of 750 nm from a mode-locked Ti: sapphire laser that produces an optical pulse train at 76 MHz; Hamamatsu synchroscan streak camera C5680 with an infrared enhanced S1 cathode was used for signal detection. The uncapped QDs surface morphology was characterized by a Veeco Nanoscope V AFM.

Results and discussion

The current density-voltage (J-V) characteristics of the Si-doped InAs QDSCs and GaAs reference SCs are presented in
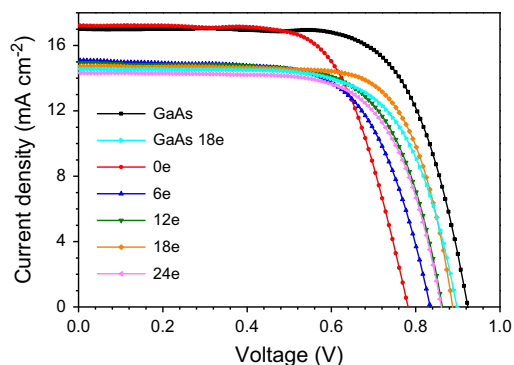
Figure 1 Current density vs. voltage measurements obtained under one Sun (AM 1.5G) illumination for Si-doped QDSCs, GaAs SC, and 18e GaAs SC.

Table 1 Fill factor, power, and efficiency measurements for Si-doped QDSCs and GaAs reference SCs extracted from the *J-V* graph in Figure 1.

Device	J_{SC} (mA cm^{-2})	V_{OC} (V)	FF (%)	η (%)
0e/dot	17.2	0.777	67.8	9.1
6e/dot	15.1	0.833	66.1	8.3
12e/dot	15.0	0.858	68.4	8.8
18e/dot	14.7	0.882	73.2	9.5
24e/dot	14.3	0.858	69.3	8.5
GaAs 18e	14.6	0.890	69.1	8.9
GaAs	17.0	0.922	70.4	11.0

Figure 1. Although there is a small increase in photocurrent for the QDSC without silicon doping, the V_{OC} is significantly reduced from 0.922 V to 0.777 V. The difference in short-circuit current density (J_{SC}) may have resulted from the optical quality of the QD/bulk interface and additional sub-bandgap absorption from QDs [15,16]. The degradation of V_{OC} has been widely observed for QDSCs, and is one of the major issues for realizing high-efficiency QD-IBSCs. Due to the shallow confinement potentials in the QDs, the thermal escape of carriers dominates at room temperature. As a result, the quasi-Fermi levels cannot be separated, which causes the reduction in V_{OC}. The *J-V* characteristics in Figure 1 also show a clear influence of doping on the performance of the solar cells (Table 1). With increasing doping, the J_{SC} gradually decreases from 17.2 mA/cm^2 for the 0e QDSC to 14.3 mA/cm^2 for the 24e QDSC. The Si dopants can substitute both Ga and As sites or exist as interstitials, forming point defects [17,18]. Therefore, the reduction of J_{SC} is attributed to defect states induced by Si-doping. This reduces the lifetime of minority carriers and consequently leads to increasing Shockley–Read–Hall recombination (R_{SRH}). At the same time, the decrease in depletion region width caused by doping that reduces the effective area for absorption could also contribute to the reduction in J_{SC}. The decrease of J_{SC} after Si doping is further substantiated by the EQE spectra in Figure 2 that shows reduced photocurrent response in the supra-band-gap region (400-900 nm) for the Si-doped SCs. To verify these assumptions, a reference GaAs solar cell with the same doping profile as the 18e QDSC, hereafter named 18e GaAs SC, was fabricated and tested. The 18e GaAs SC exhibits similar *J-V* characteristics and EQE spectrum as the 18e QDSC. Compared with the GaAs reference cell without Si doping in the intrinsic region, the J_{SC} and quantum efficiency of the 18e GaAs SC are reduced to the same magnitude of that of the 18e QDSC. This confirms that the reduction in J_{SC} of doped QDSCs has to be linked to Si dopants.

Although the increase in doping density in the QDs results in a decrease in J_{SC}, the enhancement in V_{OC} corresponds to an overall improvement in efficiency after Si doping. With increasing doping concentration in the QDs, the V_{OC} has gradually improved. The V_{OC} increases from 0.777 V for the 0e QDSC to 0.882 V, a 105 mV recovery of V_{OC} with Si-doping for the 18e QDSC. At higher doping concentrations (24e) the V_{OC} starts to diminish (Table 1), which signifies that
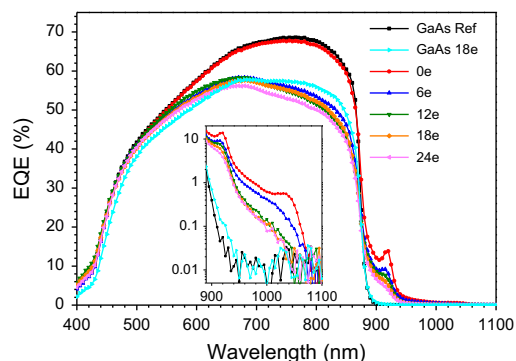

Figure 2 External quantum efficiency (EQE) spectra measured for Si-doped QDSCs, GaAs SC, and GaAs 18e. The inset shows a semi-log scale EQE that corresponds to low-energy photons absorbed by the QDs.

excessive doping increases the contribution from R_{SRH}. The recovery of V_{OC} with moderate doping density in QDs is encouraging. Such an enhancement has been attributed to saturation of the strain-induced dislocations of the QDs [19]. However, the high-growth-temperature GaAs spacer layers were used for QD growth in the current study, and strain-induced dislocations are expected to be minimized [20,21]. As shown in Figures 1 and 2, the reductions of both J_{SC} and EQE of doped QDSCs suggest a loss mechanism after the presence of dopants in the QDs. Moreover, the 18e GaAs SC shows a slight reduction instead of improvement of V_{OC} compared to the GaAs SC without doping in the intrinsic region. Therefore, the saturation of dislocations by direct doping can not be the origin of the V_{OC} recovery in the current study and the doping in the QDs more likely introduces point defects that reduce the J_{SC} instead of compensating the strain-induced dislocations. In addition, this presumption is also confirmed by low-temperature PL measurements, as shown in Figure 3a. At 10 K, the emission of the undoped QDSC is higher than that of the doped QDSCs. Because of the suppressed thermionic emission of carriers at such low temperatures, the non-radiative recombination via the mid-bandgap states is assigned as the major cause of PL reduction in the doped QDSCs [22]. On the contrary, the PL intensity increases with higher doping concentration in the QDs at room temperature (RT) (shown in Figure 3a) [23]. The enhanced emission of doped QDSCs
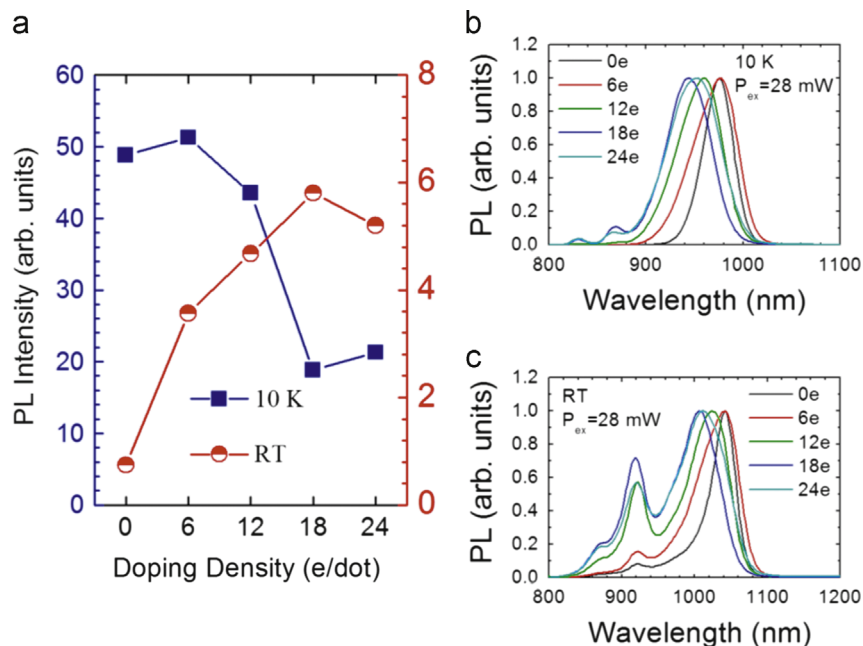
Figure 3 (a) Integrated PL intensity for Si-doped QDSCs with 0e, 6e, 12e, 18e, and 24e per QD measured at 10 K and room temperature (RT). The normalized PL spectra measured at (b) 10 K and (c) RT. The laser excitation power is 28 mW.
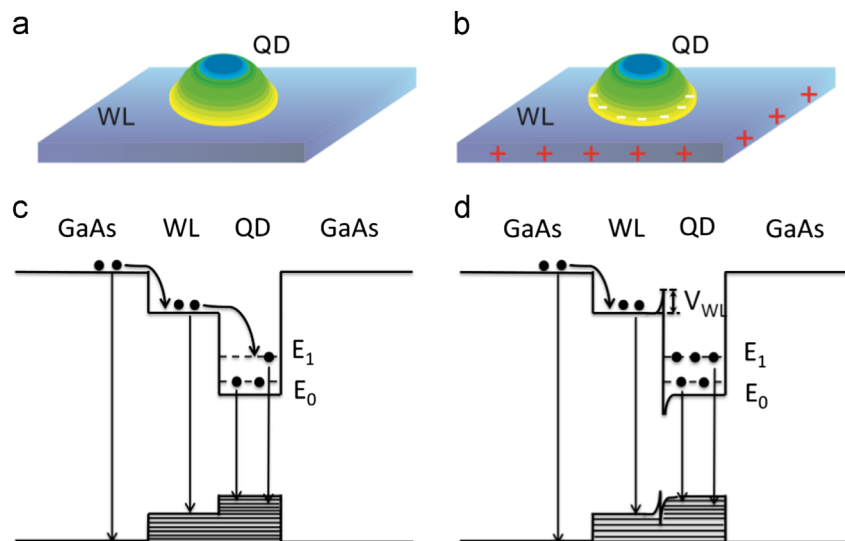

Figure 4 Illustrations of charge distribution in the QDs for (a) un-doped QDs and (b) Si-doped QDs, respectively. Schematic diagrams depict the electron relaxation pathways in InAs/GaAs QDSCs for (c) un-doped QDs and (d) Si-doped QDs, where E_0 and E_1 are the ground and first-excited states, respectively. V_{WL} is the potential barrier formed at the QD and wetting layer interface.

suggests that PL quenching is suppressed by increasing the thermal activation energy after Si doping (see Supporting information, Figure S2). The thermal activation energy can be expressed as $E_a = \Delta E_C - E_F$, where ΔE_C and E_F is the conduction-band discontinuity and the QD quasi-Fermi level, respectively [24]. This increase in thermal activation energy with doping density indicates a higher IB-CB potential separation, which could be the reason for recovered V_{OC} after doping.

It has been demonstrated that potential barriers can form around QDs in a delta-doped structure by solving

self-consistently Schrödinger and Poisson equations [25]. Even though the dopants are directly supplied to the QDs in this study, only some of the Si dopants are incorporated in the QDs and the rest remain in the WL. As shown in Figure 4, the Si dopants that remain in the WL supply free carriers to the QDs and the QDs are then filled with electrons [26,27]. As a result, a positively charged WL with ionized Si donors and negatively charged QDs is created by direct Si doping (Figure 4a and b). This is predicted to form a potential barrier V_{WL} at the WL/QD interface that increases with doping density, and subsequently suppresses electrons

thermally escaping from the QDs (Figure 4c and d) [26]. This assumption of the presence of a potential barrier agrees well with the shift of PL spectra measured at 10 K and RT (Figure 3b and c). The emission peaks from QD ground states are shown at 10 K (about 950 nm) and RT (about 1050 nm) for each Si-doped QDSC (Figure 3). The QD peaks undergo a similar blueshift at both 10 K and RT that could be attributed to the increase in quantum confinement as the Si-doping increases. The increase of doping density in the QDs induces a blueshift in the PL peak wavelength as a result of enlarged V_{WL}. In addition, a blueshift of the QD EQE, as shown in the inset in Figure 2 also points towards the possible increase in the quantum confinement of the QDs with higher doping densities due to the formation of a potential barrier.

Interestingly, this blueshift is accompanied by an increase in PL emission intensity of the WL (positioned at about 870 nm for 10 K and 920 nm for RT). Generally, as schematically shown in Figure 4c, free carriers generated in the GaAs matrix can be efficiently captured by the InAs QDs directly or via the WL through processes such as Auger scattering or multi-phonon emission [28,29]. The capture time constant is on the order of ps which is much faster than the interband radiative recombination times ($\sim$ns) [29]. Therefore, the increase in WL PL emission with increasing Si doping in the QDs evidences retarded carrier transport between the WL and QDs, leading to a portion of carriers captured by the WL recombining radiatively in the WL (Figure 4d). Excitation power dependent PL spectra give further insight into the thermal decoupling between the WL and QDs. As expected from the reduced coupling between the WL and QDs with doping, the dependence of PL spectra on the excitation power also demonstrates that the WL peak dominates over the emission from the excited states for the QDSCs with high doping densities (see Supporting information, Figure S3 and Figure S4). This signifies the presence of a potential barrier at the QD-WL interface, and provides additional evidence to support the decoupling between the WL and QDs at a high doping density. Similarly, this is also verified by the sub-bandgap EQE spectra shown in the inset of Figure 2, which shows decreasing EQE contribution

from the QDs with increasing doping density. As the doping density in the QDs increases, the sub-bandgap transition is clearly reduced. For EQE measurements with monochromatic illumination, the reduction of quantum efficiency for sub-bandgap photons is a clear indication of suppressed thermal escape of photo-excited electrons from the QDs [10,14]. It is worth noting that the increase in doping density in the QDs can also cause the Fermi level to shift towards the CB edge of GaAs, which is another possible cause for the voltage recovery and reduced interband transition in the QDs. However, the small voltage difference ($\sim$8 mV) between the 18e GaAs SC and 18e QDSC cannot be fully attributed to the shift of Fermi level with doping. Moreover, the blueshift of the EQE spectra of the QDSCs with different doping concentration is relatively small compared with the enhancement of V_{OC}, which suggests that the shift of ground states introduced by direct doping in the QDs cannot be the main reason for the significant recovery of V_{OC}. It is also possible that the increase of n-type doping in the intrinsic region shrinks the deletion region so that the quantum dot layers are mainly located outside of the deletion region. In such a case, the V_{OC} is also expected to increase. Therefore, this possibility cannot be ruled out in the current study.

All the experimental results from EQE and steady-state PL measurements suggest the voltage recovery is linked to the suppressed coupling between the WL and QDs. The critical question here is whether the voltage recovery measured at RT can be attributed to the decoupling between the WL and QDs or Si doping. As shown in the inset of Figure 2 and Figure 3c, the QD thermalization and repopulation of WL are still possible at RT, which might hinder the quasi-Fermi level split. To understand this, the transient PL spectra of the doped QDSCs were further studied at 10 K and RT, as shown in Figure 5. At 10 K, the PL decay time of the QDs is nearly constant in the range between $\sim$1.0 ns and 1.2 ns and the PL decay time of the WL significantly increases with doping density in the QDs (Figure 5b and c). In contrast, the RT PL decay time of the QDs increases with Si doping density in the QDs while the PL decay time of the WL ($\sim$150 ps) remain almost unchanged (Figure 5b and c). The enhanced low-temperature PL decay time of the WL at high
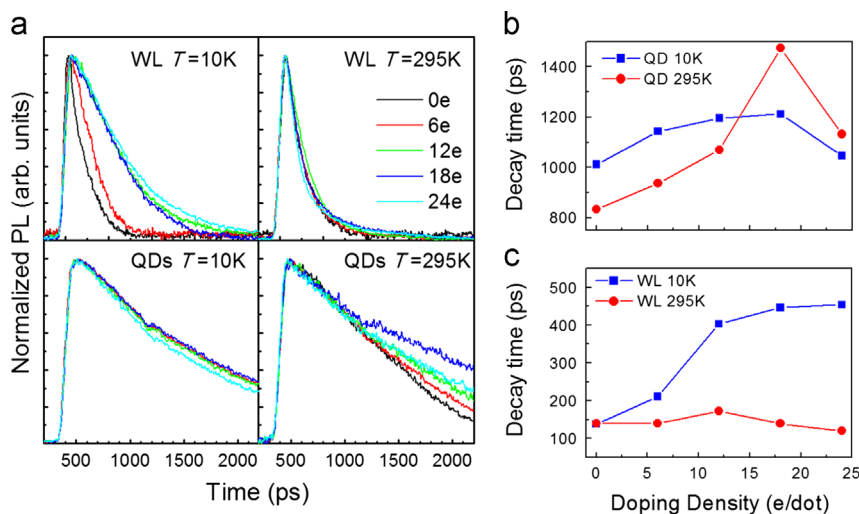

Figure 5 (a) Normalized transient photoluminescence (PL) spectra of Si-doped InAs/GaAs QDs and associated wetting layer (WL) measured at 10 K and 295 K. Photo-excited carrier decay times of the QDs in (b) and the corresponding WL in (c) measured at 10 K and 295 K.

doping concentration depicts the presence of a potential barrier at the WL/QD interface that localizes the photon-excited carriers in the WL for extended time. When the doping density reaches 24e per dot, the degradation of the crystal quality provides additional non-radiative channels for PL decay. At RT (295 K), the Si doping has negligible effects on the PL decay time of the WL because the thermalization becomes sufficient to delocalize the carriers in the WL despite the presence of a potential barrier, V_{WL}. The transient PL from the QD ground states in Figure 5a shows two decay components at RT that account for the extended decay time. The faster decay rate is independent of the doping density and correlates with relaxation from the electron ground state E_0 to the VB. The second decay rate is dependent on the doping density and shows prolonged carrier lifetime for higher doping densities. We attribute this to the potential barrier at the WL/QD interface that restricts the transition of photon-excited carriers into the QD as well as the thermalization of carriers from the QDs back into the WL and continuum (Figure 4d). This significantly prolongs the PL decay time of excited carriers in the QDs at RT as shown in Figure 5b. This effect agrees with the observed increase in thermal activation energy with doping and more importantly, confirms reduced thermal coupling between the WL and QDs even at RT (295 K).

Conclusion

In conclusion, we have demonstrated that direct Si doping in QDs leads to an improved V_{OC} as large as 105 mV. This could be explained in terms of the reduced thermal coupling of QD states from the WL and CB in GaAs QDSCs assisted by Si doping. This reduced thermal coupling could be attributed to a potential barrier formed between the WL and QDs. The formation of the potential barrier was confirmed by using EQE and steady-state PL measurements. More importantly, the transient PL measurements demonstrated a prolonged carrier lifetime in the QDs and hence suppressed thermal coupling between the QD/(WL, CB) at RT. Changes, e.g. depletion region width, in the devices structure with doping in the QDs might also be attributed to the voltage recovery, which should be kept in mind for future doped QD-IBSC design and could be also particularly important for maintaining a high short-circuit current of QDSCs. Nonetheless, the findings presented here provide an easy and important means to overcome one of the main challenges that face QD-IBSCs, and bring us a step closer to realizing the high efficiencies for QDSCs predicted by the IBSC theoretical model.

Acknowledgments

Appendix A.   Supporting information

Supplementary data associated with this article can be found in the online version at http://dx.doi.org/10.1016/j.nanoen.2014.03.016.

References

[1] A. Luque, A. Martí, Phys. Rev. Lett. 78 (1997) 5014.
[2] A. Martí, L. Cuadra, A. Luque, IEEE Trans. Electron Devices 48 (2001) 2394.
[3] A. Martí, E. Antolín, C.R. Stanley, C.D. Farmer, N. López, P. Díaz, E. Cánovas, P.G. Linares, A. Luque, Phys. Rev. Lett. 97 (2006) 247701.
[4] G. Wei, S.R. Forrest, Nano Lett. 7 (2007) 218-222.
[5] J. Wu, S.C. Mangham, V.R. Reddy, M.O. Manasreh, B.D. Weaver, Sol. Energy Mater. Sol. Cells 102 (2012) 44-49.
[6] Y. Okada, T. Morioka, K. Yoshida, R. Oshima, Y. Shoji, T. Inoue, T. Kita, J. Appl. Phys. 109 (2011) 024301.
[7] A. Luque, A. Marti, C. Stanley, Nat. Photon. 6 (2012) 146-152.
[8] A. Luque, A. Marti, Adv. Mater. 22 (2010) 160-174.
[9] S. Sanguinetti, M. Henini, M.G. Alessi, M. Capizzi, P. Frigeri, S. Franchi, Phys. Rev. B 60 (1999) 8276.
[10] E. Antolín, A. Marti, C. Farmer, P. Linares, E. Hernández, A. Sánchez, T. Ben, S. Molina, C. Stanley, A. Luque, J. Appl. Phys. 108 (2010) 064513.
[11] C.G. Bailey, D.V. Forbes, R.P. Raffaelle, S.M. Hubbard, Appl. Phys. Lett. 98 (2011) 163105.
[12] A. Mellor, A. Luque, I. Tobías, A. Martí, Adv. Funct. Mater. 24 (2014) 339-345.
[13] F. Tutu, P. Lam, J. Wu, N. Miyashita, Y. Okada, K. Lee, N. Ekins-Daukes, J. Wilson, H. Liu, Appl. Phys. Lett. 102 (2013) 043901.
[14] I. Ramiro, E. Antolín, M. Steer, P. Linares, E. Hernandez, I. Artacho, E. Lopez, T. Ben, J. Ripalda, S. Molina, in: Proceedings of the 38th IEEE Photovoltaic Specialists Conference (PVSC), 2012, pp. 000652-000656.
[15] T. Tayagaki, Y. Hoshi, N. Usami, Sci. Rep. 3 (2013) 2703.
[16] F. Tutu, J. Wu, P. Lam, M. Tang, N. Miyashita, Y. Okada, J. Wilson, R. Allison, H. Liu, Appl. Phys. Lett. 103 (2013) (043901-043901-5).
[17] D. Hurle, J. Appl. Phys. 85 (1999) 6957-7022.
[18] D. Hurle, J. Appl. Phys. 107 (2010) 121301.
[19] X. Yang, K. Wang, Y. Gu, H. Ni, X. Wang, T. Yang, Z. Wang, Sol. Energy Mater. Sol. Cells 113 (2013) 144-147.
[20] H. Liu, I. Sellers, T. Badcock, D. Mowbray, M. Skolnick, K. Groom, M. Gutierrez, M. Hopkinson, J. Ng, J. David, Appl. Phys. Lett. 85 (2004) 704-706.
[21] F. Tutu, I. Sellers, M. Peinado, C. Pastore, S. Willis, A. Watt, T. Wang, H. Liu, J. Appl. Phys. 111 (2012) 046101.
[22] J. Phillips, K. Kamath, X. Zhou, N. Chervela, P. Bhattacharya, Appl. Phys. Lett. 71 (1997) 2079-2081.
[23] T. Kita, R. Hasagawa, T. Inoue, J. Appl. Phys. 110 (2011) 103511.
[24] S. Lin, Y. Tsai, S. Lee, Appl. Phys. Lett. 78 (2001) 2784-2786.
[25] K.A. Sablon, J.W. Little, V. Mitin, A. Sergeev, N. Vagidov, K. Reinhardt, Nano Lett. 11 (2011) 2311.
[26] K. Drozdowicz-Tomsia, E. Goldys, L. Fu, C. Jagadish, Appl. Phys. Lett. 89 (2006) 113510.
[27] S. Lin, Y. Tsai, S. Lee, Jpn. J. Appl. Phys. 43 (2004) 167.
[28] T. Nowozin, L. Bonato, A. Hogner, A. Wiengarten, D. Bimberg, W. Lin, S. Lin, C. Reyner, B.L. Liang, D. Huffaker, Appl. Phys. Lett. 102 (2013) 052115.
[29] G.A. Narvaez, G. Bester, A. Zunger, Phys. Rev. B 74 (2006) 075403.

Winson Phu Minh Lam received a B.Sc degree from University College of London in 2010, followed by M.Sc in Nanotechnology in 2011. He joined the Molecular Beam Epitaxy research group at UCL in early 2012 as a Ph.D. student and is currently working on fabrication of III-V Semiconductor Quantum Dot Solar Cells.

Sabina Hatch is currently a postdoctoral research associate in the Department of Electrical and Electronic Engineering at University College London. She received her Masters in Science (Physics) from Bristol University, UK and completed her Ph.D. in Material Science at Queen Mary University of London, UK in 2013. Her research focuses on the fabrication of purely-inorganic and inorganic-organic hybrid optoelectronic devices using low-dimensional III-V structures (i.e. quantum well, quantum dots, and quantum nanowires).

Jiang Wu received his B.S. degree from University of Electronic Science and Technology of China, and M.S. and Ph.D. degrees from the University of Arkansas-Fayetteville, USA, in 2008 and 2011 respectively. He is currently a research associate in the Department of Electrical and Electronic Engineering at University College London. His research interests include Molecular Beam Epitaxy growth and optoelectronic devices, including photovoltaic cells, lasers and photodetectors.


Mingchu Tang received a B.Eng degree in Electronic and Electrical Engineering in University of Sussex, UK, in 2011. He is currently a PhD student in University College London, UK. His current research interest includes III-V quantum-dot materials and devices and Molecular Beam Epitaxy growth.

Vitaliy G. Dorogan received the B.S. and M.S. degrees in physics from the Physics Department, Uzhgorod State University, Uzhgorod, Ukraine, in 1999 and 2000, and the Ph.D. degree respectively in microelectronics-photonics from the University of Arkansas, Fayetteville, in 2011. He is currently a Research Assistant Professor at Institute for Nanoscience and Engineering, University of Arkansas, Fayetteville. His current research interests include the spectroscopic study of semiconductor nanostructures.

Yuriy Mazur reseived a M.Sc in Solid State Physics from. Moscow Institute of Physics and Engineering in 1978, and Ph.D in Solid State Physics from Institute of General Physics, Moscow, USSR in 1983. He worked at the Institute of Semiconductors Physics, National Academy of Sciences, Kiev, Ukraine and Max-Born-Institute Berlin, Germany as a Senior Research Associate and Visiting Scientist during 1982-2000. He joined the Department of Physics, University of Arkansas in 2001, and currently holds the position as a Research Professor at the Institute for Nanoscience and Engineering University of Arkansas Fayetteville, USA. His research interests include physics of magnetic phenomena and disordering in the semimagnetic semiconductors, physics of two-dimensional electron (hole) states and excitons in III-V semiconductor heterostructures and quantum dots.
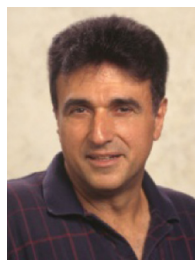
Gregory J. Salamo received a Ph.D. degree in physics from the City University of New York, New York, in 1973. He was an Intern Student at Bell Laboratories, Murray Hill, NJ. He was a Postdoctoral Researcher at the Institute of Optics, University of Rochester, Rochester, NY. In 1975, he joined the faculty of the University of Arkansas, Fayetteville, where he is currently a Distinguished Professor of physics. He is the Co-Director of the National Science Foundation (NSF) Materials Research Science and Engineering Center on the physics of semiconductor nanostructures. He has published more than 300 papers in referred journals, given numerous contributed and invited talks, and contributed several book chapters. He has carried out research in the areas of optical communications, optical image processing, and the optical properties of semiconductors. He is involved in the development of interdisciplinary research and education through the establishment of a new degree program to provide greater career opportunities for students and faculty. He is also involved in the development of an educational course and laboratory in nanotechnology and a GK-12 NSF program for middle school students. His research is currently focused on growing III-V semiconductors and ferroelectrics using molecular beam epitaxy and scanning tunneling microscopy. Dr. Salamo is a Fellow of the Optical Society of America.


Íñigo Ramiro received a Engineering degree in telecommunication from the Universidad Politécnica de Madrid (UPM), Madrid, Spain, and from the Institut National des Télécommunications, Evry, France, in 2008. He is currently working toward the Ph.D. degree with the Instituto de Energía Solar, Escuela Técnica Superior de Ingenieros de Telecomunicación, UPM, Madrid, in the development and characterization of intermediate band solar cells from which he has a UPM Doctoral Grant.

Alwyn J. Seeds received a B.Sc., Ph.D. and D.Sc. degrees from the University of London. In 1980 he was appointed a Staff Member at Lincoln Laboratory, Massachusetts Institute of Technology, where he worked on GaAs monolithic millimetre-wave integrated circuits for use in phased-array radar. He returned to England in 1983 to take up a lectureship at Queen Mary College, University of London, moving to University College London in 1986,

where he is now Professor of Opto-electronics and Head of the Department of Electronic and Electrical Engineering. He has published over 400 papers on microwave and opto-electronic devices and their systems applications. His current research interests include III-V semiconductor devices, optical frequency synthesis, broadband wireless over fiber access systems, coherent optical networks, THz photonics and non-linear optical devices. Professor Seeds has been elected a Fellow of the Royal Academy of Engineering (UK) and an IEEE Fellow (USA). He has been a Member of the Board of Governors and Vice-President for Technical Affairs of the IEEE Photonics Society (USA). He has served on the programme committees for many international conferences. He is a co-founder of Zinwave, a manufacturer of wireless over fibre systems and founder of PhronTera, a manufacturer of ultra-fast photonic devices and systems.
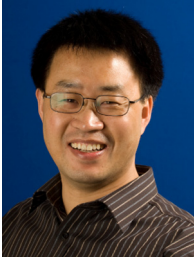
Huiyun Liu received a PhD in Semiconductor Science from the Institute of Semiconductor, Chinese Academy of Sciences. After receiving his PhD, he joined the EPSRC National Centre for III–V Technologies at University of Sheffield in August 2001. In 2007, he was awarded Royal Society University Research Fellow and joined the Department of Electronic and Electrical Engineering at University College London,

UK, where he is now a Professor of Semiconductor Photonics. He has been working on the development of III-V compound materials and devices. His current research interest concentrates on the nano-metre-scale engineering of low-dimensional semiconductor structures (such as quantum dots, nanowires, and quantum wells) by using molecular beam epitaxy and the development of novel optoelectronic devices including solar cells, lasers, detectors, and modulators by developing novel device process techniques.